Investigation of a hydrogen implantation-induced blistering phenomenon in $Si_{0.70}Ge_{0.30}$

2011 Semicond. Sci. Technol. 26 125001

(http://iopscience.iop.org/0268-1242/26/12/125001)

Semicond. Sci. Technol. 26 (2011) 125001 (5pp) doi:10.1088/0268-1242/26/12/125001

Investigation of a hydrogen implantation-induced blistering phenomenon in $Si_{0.70}Ge_{0.30}$

R Singh[1,2], R Scholz[2], S Christiansen[2,4], S Mantl[3] and M Reiche[2]

[1] Department of Physics, Indian Institute of Technology Delhi, Hauz Khas, New Delhi -110 016, India
[2] Max Planck Institute of Microstructure Physics, Weinberg 2, Halle 06120, Germany
[3] Institute of Bio- and Nanosystems (IBN-1), Forschungszentrum Juelich and JARA- Fundamentals of Future Information Technology, 52425 Juelich, Germany

E-mail: rsingh@physics.iitd.ac.in

Received 10 July 2011, in final form 11 September 2011
Published 26 October 2011
Online at stacks.iop.org/SST/26/125001

Abstract
The blistering phenomenon in hydrogen implanted and annealed $Si_{0.70}Ge_{0.30}(0\,0\,1)$ layers was investigated. The implantation was performed with 240 keV H_2^+ ions with a fluence of 5×10^{16} cm^{-2}. The blistering kinetics of H-implanted $Si_{0.70}Ge_{0.30}$ showed two different activation energies: about 1.60 eV in the lower temperature regime (350–425 °C) and 0.40 eV in the higher temperature regime (425–700 °C). Microstructural characterization of the implantation damage in SiGe layers using transmission electron microscopy revealed a damage band extending between 900 and 1200 nm below the surface. It was observed that after post-implantation annealing, a number of platelets and microcracks were formed within the damage band. These extended defects are predominantly oriented parallel to the surface, i.e. in the (0 0 1) plane. However, the extended defects oriented along the {1 1 1} planes were also observed and the density of these defects was the highest toward the end of the damage band. These experimental observations are compared with similar investigations in Si and Ge performed earlier and a plausible explanation for the blistering results in $Si_{0.70}Ge_{0.30}$ is presented in this work.

1. Introduction

Strain-relaxed SiGe layers grown on Si substrates are used as templates for the growth of ultrathin strained silicon (sSi) layers [1–5]. The strain in the sSi layers depends upon the Ge content of the strain-relaxed SiGe layers, which in turn leads to enhancement in the electron mobility of up to two times higher than that of normal bulk silicon [5]. Moreover, the transfer of these ultrathin sSi layers onto oxidized silicon wafers using hydrogen implantation in the SiGe and direct wafer bonding method (ion-cut process) results in the fabrication of strained-silicon-on insulator (sSOI) substrates [6–9]. The sSOI substrates combine the benefits of enhanced carrier mobilities of sSi and low parasitics of SOI technology for nanoCMOS applications. The sSOI wafers up to 200 mm in diameter are now available [9, 10]. In the ion-cut process, hydrogen is implanted into the SiGe layer and the post-implantation annealing causes the fracture within the implanted zone [11–13]. In case the implanted wafer is bonded to an oxidized Si wafer acting as a mechanical stiffener, the thin layer is transferred onto this wafer. Otherwise dome-shaped blisters or craters are observed on free surfaces. The physical mechanisms involved in the layer splitting or blistering processes are the same. Hence, it is of great interest to study the mechanisms behind the layer splitting process, which can be carried out more conveniently by studying the development of surface blisters in hydrogen-implanted and annealed but unbonded wafers.

In the past, many investigations were carried out concerned with the blistering or splitting process in hydrogen-implanted and annealed Si wafers [11–14], but only a few studies exist for the case of Ge and SiGe alloy semiconductors [15–19]. Ngyuven *et al* studied the splitting kinetics

[4] Presently at the Max Planck Institute for the Science of Light, Günther Scharowsky Str. 1, Erlangen, Germany.

in H-implanted SiGe having 20% and 30% Ge content, respectively, and found that the activation energies for these semiconductors depend upon the hydrogen fluence used for implantation [16]. They also investigated the microstructural defects existing inside the implantation damage zone in SiGe using transmission electron microscopy (TEM). Singh *et al* studied the blistering kinetics of 22% Ge content SiGe layers using fixed implantation fluence and observed two different activation energies for the blistering in this material [17]. However, for SiGe having 30% Ge content, detailed blistering studies after H-implantation and annealing are rather scarce. Moreover, the similarities and differences observed with similar studies in Si have not been highlighted previously. In this work, we have carried out detailed studies on the H-implantation-induced blistering process in SiGe (30% Ge) using various techniques and have compared the results with the similar studies done in the case of Si and Ge, respectively.

2. Experimental details

Strain-relaxed $Si_{0.70}Ge_{0.30}$ epitaxial layers were grown on 200 mm diameter Si(0 0 1) substrates using reduced pressure chemical vapor deposition at a nominal pressure of 3.95×10^{-2} Pa (30 Torr). A commercially available Applied Materials' Centura Epi system was used for this purpose. First a 3 μm linearly graded buffer layer (with a 10% μm^{-1} Ge content increase) was grown on a Si(0 0 1) substrate, and then followed by a 2 μm uniform composition strain-relaxed $Si_{0.70}Ge_{0.30}$ layer. The SiGe wafer was implanted with 240 keV H_2^+ ions with a fluence of 5×10^{16} cm^{-2}. After hydrogen implantation the wafer was cut into small pieces of about 5×5 mm^2 size and these pieces were annealed in an ambient atmosphere furnace at various temperatures in the range of 300–700 °C in order to determine the time for blister formation on the surface at each temperature. The surface blisters were observed using an optical microscope operated in the Nomarski contrast mode. The hydrogen profile in the implanted SiGe layer was determined using secondary ion mass spectrometry (SIMS). TEM was used to study the microstructure of the implantation damage zone in SiGe. The TEM measurements were carried out using a Philips CM20T microscope operated at 200 kV.

3. Results and discussion

A typical optical image of the blisters or craters formed on the surface of SiGe after post-implantation annealing is shown in figure 1. The lateral size of the dome-shaped blisters is in the range of about 8–55 μm. Moreover, in some areas the craters are also formed and their bottom surface is found to be quite rough. The craters are formed due to the excessive pressure of the molecular hydrogen trapped within the mirocracks (as shown later) that leads to the lift-off of the top layer of SiGe. In our previous report on blistering studies in SiGe with 22% Ge content under the same implantation conditions, a similar kind of blistering image was observed but in that case the lateral size of the blisters was in the range of about 7–25 μm [17]. Hence, it can be seen that an increase in the upper limit of

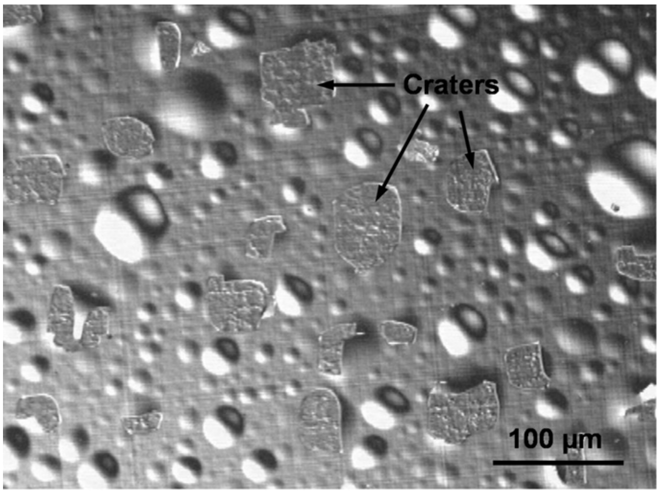

Figure 1. Nomarski optical micrograph of the surface of hydrogen-implanted $Si_{0.70}Ge_{0.30}$ layer after annealing at 500 °C for 10 min. The implantation was carried out using 240 keV H_2^+ ions with a fluence of 5×10^{16} cm^{-2}. Exfoliated areas or craters are also seen on the surface.

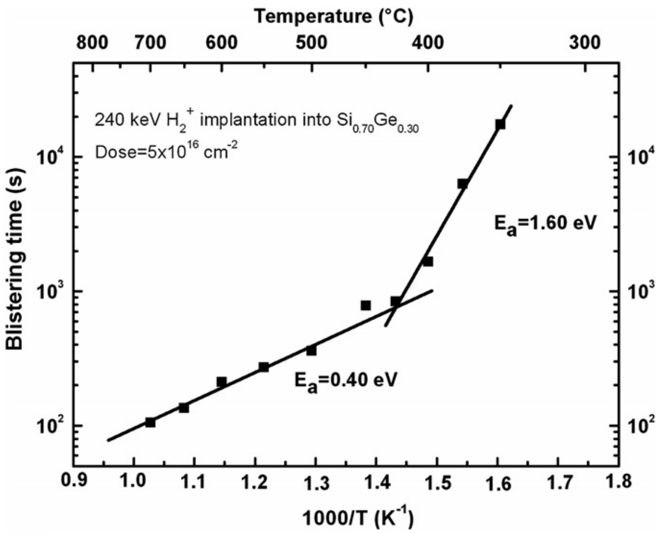

Figure 2. Arrhenius plot of the blistering time as a function of the annealing temperature for the hydrogen-implanted $Si_{0.70}Ge_{0.30}$ layer using 240 keV H_2^+ ions with a fluence of 5×10^{16} cm^{-2}.

the size of blisters is observed with an increase in Ge content from 22% to 30%. Usually under similar implantation and annealing conditions, it is observed that Ge shows larger size blisters in comparison to those in Si. So the observation of the larger size of blisters in 30% Ge content SiGe layers in comparison to those of 22% SiGe layers is quite consistent.

The blistering time at each temperature was determined optically and the graph between the blistering time and reciprocal temperature, i.e. the Arrhenius plot, is shown in figure 2. It can be clearly seen that two different activation energies are observed in the plot: about 1.60 eV in the lower temperature regime of 350–425 °C and 0.40 eV in the higher temperature regime of 425–700 °C. A similar kind of blistering kinetics behavior has been observed in some earlier studies also for Si, Ge and SiGe [17, 18–21]. It was reported by

Aspar *et al* that in the case of H-implanted Si(1 0 0) with a fluence of 6 × 10^{16} H^+ cm^{-2}, two activation energies for the splitting process were observed: 0.50 eV at the higher temperatures and 2.2 eV in the lower temperature regime [20]. The lower activation energy was related to the free atomic hydrogen diffusion in Si, while the higher activation energy was associated with the hydrogen diffusion limited by the trapping–detrapping of hydrogen. Weldon *et al* reported that the blistering activation energy was about 1.8 eV and suggested that it could be associated with the Si–Si bond energy in the lattice [12]. In a detailed study of the blistering kinetics in H-implanted Si and Ge, Bedell *et al* showed that for Si the blistering activation energy is fluence dependent (varied between 1.0 and 2.5 eV for fluence values in the range of 6 × 10^{16}–10 × 10^{16} H^+ cm^{-2}) [15]. However, for Ge the activation energy was about 1.75 eV and it was found to be almost independent of the fluence. They suggested that the above-mentioned activation energies could be associated with the Si–Si and Ge–Ge bond energies, respectively. Recently, Nguyen *et al* showed that for H-implanted SiGe, two activation energies were obtained and the higher activation energy was found to be fluence dependent [16]. Singh *et al* first reported the blistering kinetics of SiGe with 22% Ge content implanted with a fluence of 1 × 10^{17} H^+ cm^{-2} [17]. In the low-temperature regime (300–400 °C) activation energy of 1.2 eV was obtained, while in the high-temperature regime (400–700 °C) the activation energy was 0.38 eV. In the present case involving H-implantation of $Si_{0.70}Ge_{0.30}$ two activation energies are also obtained: 0.40 eV in the higher temperature regime and 1.60 eV in the lower temperature regime. The lower activation energy is close to the activation energy for diffusion of free hydrogen in Si (0.50 eV) and also in Ge (0.38 eV) [21, 22]. SiGe is an alloy semiconductor and hence we may expect the hydrogen diffusion activation energy to have a value between 0.50 and 0.38 eV, depending upon the Ge content in SiGe. We mentioned earlier that the higher blistering activation energy in $Si_{0.70}Ge_{0.30}$ was found to be 1.60 eV. Ngyuven *et al* found the value of the higher activation energy to be 2.0 eV but the hydrogen fluence was 6 × 10^{16} H^+ cm^{-2}, which is lower than the fluence that we used, i.e. 1 × 10^{17} H^+ cm^{-2} (it is to be noted that implantation with 240 keV H_2^+ ions with a fluence of 5 × 10^{16} cm^{-2} is equivalent to implantation with 120 keV H^+ ions with a fluence of 1 × 10^{17} cm^{-2}). Hence, similar to the case in pure Si [16], it is expected that we get lower activation energy for $Si_{0.70}Ge_{0.30}$. This activation energy of 1.6 eV is significantly smaller than the Si–Si (3.4 eV) and Ge–Ge (2.8 eV) bond energies. According to the trapping–detrapping phenomena observed in the case of Si [20, 23], here also the higher activation energy could be related to the hydrogen diffusion limited by trapping–detrapping in SiGe. It is worth mentioning that the Si–H and Ge–H bond energies are about 2.5 and 1.9 eV, respectively [24].

The hydrogen depth profiling in the $Si_{0.70}Ge_{0.30}$ layer implanted by 240 keV H_2^+ ions (which is equivalent to implantation with 120 keV H^+ ions) was performed using SIMS. The hydrogen depth profile is shown in figure 3 for the as-implanted SiGe sample as well as for the annealed sample

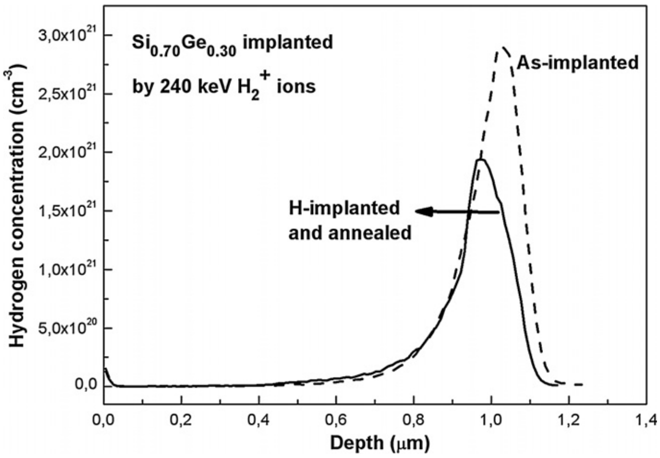

Figure 3. SIMS profiles of hydrogen in $Si_{0.70}Ge_{0.30}$ in the as-implanted and annealed states.

(annealing at 500 °C for 5 min). In the as-implanted state, the peak hydrogen concentration was close to 3.0 × 10^{21} cm^{-3} and was located at a depth of 1060 nm below the surface. This agrees very well with the depth of peak hydrogen concentration as calculated using the SRIM2010 simulation program [25], which is about 1050 nm. After the post-implantation annealing, the peak hydrogen concentration was reduced to about 2.0 × 10^{21} cm^{-3} and its position shifted toward the surface at 980 nm. Moreover, the hydrogen distribution also became narrower. Similar observations were recently made by Personnic *et al* in the case of H-implanted Si [26], where they observed that after post-implantation annealing, the peak concentration got reduced and the hydrogen distribution became narrower (the annealing temperature was up to 400 °C). They showed that the reduction in the SIMS signal after annealing was not due to the outdiffusion of hydrogen from the implanted region but to some rearrangement of the hydrogen atoms in a form not detectable by SIMS [26]. This kind of behavior in SiGe, as in the case of Si, is due to the trapping of hydrogen by the vacancies and the internal surfaces of platelets that are formed during the annealing process. Moreover, a portion of the implanted hydrogen tends to transform to the molecular hydrogen form that is trapped within the platelets [26]. Since the maximum implantation damage exists somewhat shallower than the peak of hydrogen concentration, after annealing the hydrogen preferentially moves toward the damaged region leading to a shift in the peak of hydrogen concentration.

The microstructural characterization of the implantation-induced damage was performed using TEM, and the cross-sectional transmission electron microscopy (XTEM) image of the SiGe layer in the as-implanted state is shown in figure 4. A damage band could be observed ranging from about 920 to 1200 nm below the surface. The damage band consists of defects such as vacancies, interstitials and vacancy–hydrogen complexes that are created due to the energetic hydrogen ions. An XTEM image of the annealed SiGe sample is shown in figure 5, which shows the formation of two-dimensional extended defects such as platelets and small area microcracks. The density of the (0 0 1) oriented platelets and the microcracks

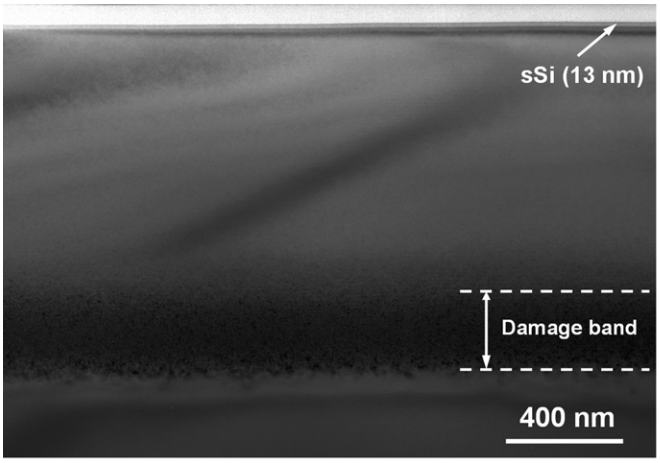

Figure 4. Cross-sectional transmission electron microscopy (XTEM) image of the hydrogen-implanted and annealed (500 °C for 5 min, i.e. just below the blistering time) $Si_{0.70}Ge_{0.30}$ layer.

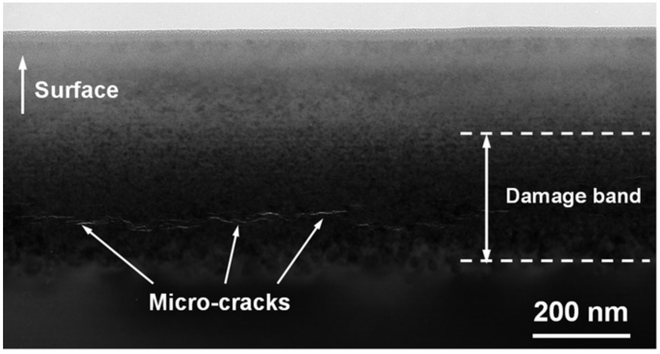

Figure 5. Higher magnification XTEM image of the hydrogen-implanted and annealed (500 °C for 5 min) $Si_{0.70}Ge_{0.30}$ layer. The (0 0 1) platelets and small microcracks are clearly observed in the damage band.

is found to be the maximum within a narrow range of about 100 nm within the damage band. Moreover, the microcracks are lying mostly parallel to the (0 0 1) surface and they are randomly joined to each other by some microcracks lying along {1 1 1} planes. The hydrogen passivates and gets trapped in the internal surfaces of the platelets [12]. Moreover, a portion of the total hydrogen exists in the form of molecular hydrogen, H_2, filled inside the open volume of the platelets. The H_2 gas exerts pressure inside them upon annealing leading to the formation of microcracks. If the annealing is continued for longer times, these microcracks grow in size leading eventually to the formation of surface blistering [13]. The (0 0 1) oriented platelets and microcracks could be seen more clearly in the higher magnification TEM image in figure 6. While the density of the (0 0 1) platelets is higher inside the damage band, there are some {1 1 1} oriented platelets also, which are found relatively in more abundance at the end of the damage band. Recently, this kind of behavior of platelet formation in hydrogenated Si was studied by Swadener *et al* using molecular dynamics (MD) simulations [27] and they showed that when there is a biaxial compressive stress in the (1 0 0) plane in Si, then the (1 0 0) platelets are formed in the region of highest stress at the center of implantation damage,

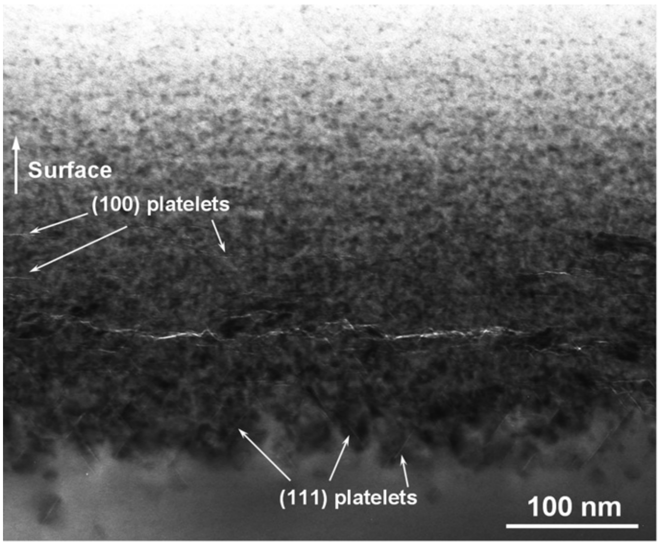

Figure 6. Higher magnification XTEM image of the hydrogen-implanted and annealed (500 °C for 5 min) $Si_{0.70}Ge_{0.30}$ layer. Apart from the (0 0 1) platelets and small microcracks, {1 1 1} platelets existing predominantly at the end of the damage band are also observed.

while (1 1 1) platelets form in the lower stress regions at the end of the damage band. In the case of H-implanted $Si_{0.70}Ge_{0.30}$ having (0 0 1) surface orientation, the biaxial compressive stress is the highest near the mid of the damage band and hence (0 0 1) platelets are preferentially formed in that region of the damage band. Moreover, in accordance with the MD simulation studies, we also found experimentally that the {1 1 1} platelets are preferentially located at the end of the damage band.

4. Conclusions

The blistering phenomenon in hydrogen-implanted and annealed SiGe(0 0 1) layers with 30% Ge content was investigated. The blistering kinetics in SiGe showed two activation energies. These activation energies were associated with the diffusion activation energies of atomic hydrogen in the damaged lattice of SiGe. The depth distribution of hydrogen after post-implantation annealing became slightly narrower and shifted toward the surface in comparison with that of the as-implanted state. This indicated that the hydrogen was getting trapped inside the platelets and microcracks. The TEM measurements showed the existence of a damage band, which after annealing showed a number of (0 0 1) platelets and microcracks. A number of {1 1 1} platelets were also observed preferentially at the end of the damage band. In accordance with earlier reported MD simulation studies, the implantation-induced biaxial compressive stress in the damage band led to the preferential existence of (0 0 1) and {1 1 1} platelets at the center and the end of the damage band, respectively.

Acknowledgments

The authors are thankful to S Hopfe for XTEM specimen preparation. The work is supported financially by the

Max Planck Society (MPS), Germany under the cooperation scheme of Max Planck India Partner Group and co-funded by the Department of Science and Technology (DST), India. We gratefully acknowledge Dr D Webb, formerly at ATMI Epitaxial Services Inc., AZ, USA for providing SiGe virtual substrates for our experiments. We are thankful to Dr Oussama Moutanabbir from the Max Planck Institute of Microstructure Physics, Halle, Germany for many useful discussions. We are ever grateful to late Professor U Gösele who always inspired us and pioneered the area of wafer bonding and ion-cut studies in semiconductors.

References

[1] Currie M T, Leitz C W, Langdo T A, Taraschi G, Antoniadis D A and Fitzgerald E A 2001 *J. Vac. Sci. Technol.* B **19** 2268
[2] Lee M L, Pitera A J and Fitzgerald E A 2004 *J. Vac. Sci. Technol.* B **22** 158
[3] Buca D, Höllander B, Trinkaus H, Mantl S, Carius R, Loo R, Caymax M and Schaefer H 2004 *Appl. Phys. Lett.* **85** 2499
[4] Bedell S W, Fogel K, Sadana D K, Chen H and Domenicucci A 2004 *Appl. Phys. Lett.* **85** 2493
[5] Hartmann J M, Abbadie A, Rouchon D, Mermoux M and Billon T 2007 *Semicond. Sci. Technol.* **22** 362
[6] Langdo T A *et al* 2003 *Appl. Phys. Lett.* **82** 4256
[7] Ghyselen G *et al* 2004 *Solid-State Electron.* **48** 1285
[8] Christiansen S H, Singh R, Radu I, Reiche M, Gösele U, Webb D, Bukalo S and Dietrich B 2005 *Mater. Sci. Semicond. Process.* **8** 197
[9] Reiche M *et al* 2007 *Electrochem. Soc. Trans* **6** 339
[10] www.soitec.com
[11] Bruel M 1995 *Electron. Lett.* **31** 1201
[12] Weldon M K *et al* 1997 *J. Vac. Sci. Technol.* B **15** 1065
[13] Höchbauer T, Misra A, Nastasi M and Mayer J W 2001 *J. Appl. Phys.* **89** 5980
[14] Terreault B 2007 *Phys. Status Solidi* a **204** 2129
[15] Bedell S W and Lanford W A 2001 *J. Appl. Phys.* **90** 1138
[16] Nguyen P *et al* 2005 *Proc. Electrochem. Soc.* 2005–03 p 185
[17] Singh R, Radu I, Reiche M, Scholz R, Webb D, Gösele U and Christiansen S H 2005 *Mater. Sci. Eng.* B **124–5** 162
[18] Desrosiers N, Giguere A, Terreault B, Chicoine M and Schiettekatte F 2008 *Nucl. Instrum. Methods Phys. Res.* **266** 1971
[19] Mazen F, Tauzin A, Sanchez L, Chieux F, Deguet C, Augendre E, Akatsu T, Richtarch C and Clavelier L 2008 *AIP Conf. Proc.* **1066** 217
[20] Aspar B *et al* 2001 *J. Electron. Mater.* **7** 834
[21] Hurley R E, Wadsworth H and Gamble H S 2007 *Vacuum* **81** 1207
[22] Tong Q-Y, Gutjahr K, Hopfe S, Gösele U and Lee T H 1997 *Appl. Phys. Lett.* **70** 1390
[23] Pearton S J, Corbett J W and Shi T S 1987 *Appl. Phys.* A **43** 153
[24] Myers S M, Stein H J and Follstaedt D M 1995 *Phys. Rev.* B **51** 9742
[25] www.srim.org
[26] Personnic S, Bourdelle K K, Letertre F, Tauyin T, Cherkashin N, Claviere A, Fortunier R and Klocker H 2008 *J. Appl. Phys.* **103** 0235508
[27] Swadener J G, Basked M I and Nastasi M 2006 *Phys. Rev.* B **72** 201202